



Cite this: *Chem. Commun.*, 2016, 52, 3058

Received 21st December 2015,
Accepted 18th January 2016

DOI: 10.1039/c5cc10455f

www.rsc.org/chemcomm

Crystallographic insights into $(\text{CH}_3\text{NH}_3)_3(\text{Bi}_2\text{I}_9)$: a new lead-free hybrid organic–inorganic material as a potential absorber for photovoltaics†

Kai Eckhardt, Volodymyr Bon, Jürgen Getzschmann, Julia Grothe, Florian M. Wisser and Stefan Kaskel*

The crystal structure of a new bismuth-based light-absorbing material for the application in solar cells was determined by single crystal X-ray diffraction for the first time. $(\text{CH}_3\text{NH}_3)_3(\text{Bi}_2\text{I}_9)$ (MBI) is a promising alternative to recently rapidly progressing hybrid organic–inorganic perovskites due to the higher tolerance against water and low toxicity. Single crystal X-ray diffraction provides detailed structural information as an essential prerequisite to gain a fundamental understanding of structure property relationships, while powder diffraction studies demonstrate a high degree of crystallinity in thin films.

In recent years a new class of light-absorbing materials, consisting of hybrid organic–inorganic perovskites (HOIPs), has gained tremendous attention. An editorial article published in nature materials in 2014 describes a “perovskite fever” among scientists, raising the hope that these materials might revolutionize the photovoltaic sector.¹ This substance class has a three-dimensional inorganic backbone and organic cations in cuboctahedral cavities.^{2–4} The basic structure of the materials mainly used in the literature is $\text{CH}_3\text{NH}_3\text{MX}_3$ (M = Sn, Pb and X = Cl, Br, I).^{2,5} These hybrid perovskites show a direct and tunable bandgap. They feature very good charge carrier mobility, high absorption coefficients and tailored electronic characteristics.^{6,7} The cells currently discussed in the literature show energy conversion efficiencies up to 20% proving their huge potential as an alternative to industrially produced solar cells.⁸ However, decisive drawbacks impede further industrial development: (1) current perovskite solar cells are based on lead and thus will fall under the category of hazardous substances with restricted use in the European Union. (2) Alternatives based on tin show a poor stability under atmospheric conditions.

Bismuth based materials could be a promising and environmentally friendly alternative. In our search for new bismuth-based

materials we discovered a new methyl ammonium iodobismuthate ($(\text{CH}_3\text{NH}_3)_3\text{Bi}_2\text{I}_9$, in the following abbreviated as MBI) with an open circuit voltage of 800 mV in a PV cell.⁹

In parallel Park *et al.* presented a similar material as an absorber with an initial efficiency of 0.12%.¹⁰

A recent workshop in February 2015 revealed that the technological advances measured by power conversion efficiencies have proceeded much more quickly than the basic physics and chemistry necessary to understand the materials.¹¹ In this context in our current study we focus on detailed insights into the crystal structure of a new iodobismuthate and correct space group assignment. It should be mentioned that single crystals of MBI were obtained by Jakubas *et al.* for the first time but Weissenberg photographs only allowed to suggest the space group $P6_3/mmc$.^{12–14} However, Park *et al.* assigned their diffraction data incorrectly to a PDF number from the ICSD data base corresponding to a guanidinium salt crystallizing in $Cmcm$ with completely different cell parameters.¹⁰

Since the correct crystal structure of MBI has not been reported yet, we synthesized crystals suitable for single crystal X-ray diffraction studies. Starting solutions of methyl ammonium iodide and bismuth(III)iodide in dimethyl-formamide (DMF) in a ratio of 3 : 1 were used in the synthesis. The red single crystals suitable for single crystal X-ray diffraction were grown using a layer crystallization technique by separating the two starting solutions of methyl ammonium iodide and bismuth(III)iodide with dichloromethane. The single crystal X-ray diffraction study confirmed initial observations of Jakubas *et al.* and the crystal structure was successfully solved in the $P6_3/mmc$ space group. The structure contains one independent Bi1 atom, located on the 3-fold axis (4f Wyckoff position) showing slightly distorted octahedral ligand coordination geometry (Fig. 1a and Table S1, ESI†). Two Bi atoms in the anion are coordinated by three symmetrically equivalent bridging I1 atoms (12j Wyckoff position) and terminal I2 atoms (12k Wyckoff position), both located on different mirror planes. The complex anion consists of two face-sharing octahedra, which are separated by methylammonium ions, which is a quite different situation compared with the corner sharing octahedra in

Department of Inorganic Chemistry, Technische Universität Dresden Bergstrasse 66, D-01069 Dresden, Germany. E-mail: stefan.kaskel@chemie.tu-dresden.de

† Electronic supplementary information (ESI) available: Synthetic details, single crystal X-ray structure analysis details. CCDC 1433118. For ESI and crystallographic data in CIF or other electronic format see DOI: 10.1039/c5cc10455f



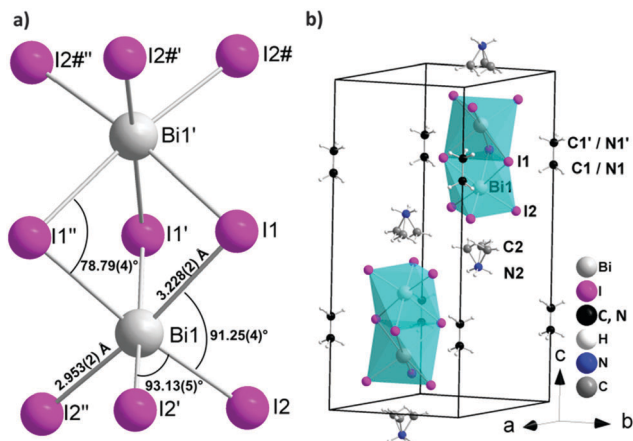


Fig. 1 Crystal structure of $(\text{CH}_3\text{NH}_3)_3\text{Bi}_2\text{I}_9$ (MBI): (a) local structure of the $\text{Bi}_2\text{I}_9^{3-}$ anion; (b) cation and anion positions in the unit cell.

the perovskite structure observed for HOIPs such as methyl ammonium lead iodide.¹⁵ A minor distortion in the BiI_6 octahedra most probably originates from the repulsion of the Bi^{3+} ions in the $\text{Bi}_2\text{I}_9^{3-}$ cluster with a $\text{Bi}\cdots\text{Bi}$ distance of $4.099(1)$ Å. This repulsion causes a slight deviation from octahedral angles, a contraction for the bridging $\text{I1}-\text{Bi1}-\text{I1}'$ (84°) and a widened $\text{I2}-\text{Bi1}-\text{I2}'$ angle (93°) (Table S2, ESI[†]). Slightly longer $\text{Bi}-\text{I1}-\text{Bi}$ bridges ($3.229(2)$ Å) are observed as compared to terminal $\text{Bi}-\text{I2}$ bonds ($2.953(2)$ Å) as expected. In the crystal structure the anions are aligned along the c axis (Fig. 1b). The interanionic $\text{I}\cdots\text{I}$ distances range from $4.263(2)$ to $4.318(2)$ Å and are thus comparable to interlayer $\text{I}\cdots\text{I}$ contacts in elemental I_2 (4.27 Å) providing a hint for potential charge transport paths. The local structure of the $\text{Bi}_2\text{I}_9^{3-}$ as well as location in the unit cell is comparable with the crystal structure of tetramethylammonium bismuth iodide $[(\text{CH}_3)_4\text{N}]_3\text{Bi}_2\text{I}_9$, crystallizing in the space group $P31c$.¹⁶ Because of the high symmetry of the unit cell and large difference between the scattering factors of Bi, I atoms and C, N atoms, the localization of the C and N atoms in the methylammonium cation is blurred. Both crystallographically independent cations are located on the 3-fold axis showing different type of disorder. The methyl ammonium cation (MA1) contains symmetrically equivalent C1 and N1 atoms located on the 3-fold axis close to the inversion center. In MA1 the position of the carbon and nitrogen atoms are indistinguishable causing substitutional disorder. MA2 involves two symmetrically distinguishable atoms, one of which (presumably nitrogen, N2) is located on the 3-fold axis. Another atom (presumably carbon, C2) is disordered occupying three symmetrically equivalent positions in vicinity to the 3-fold axis.

MBI has excellent absorbing properties (Fig. 2). Absorption spectra measured between 250 and 900 nm reveal an optical bandgap of the material at 1.94 eV as it was derived from a Tauc plot. This value is slightly higher than observed for BiI_3 with an indirect and direct bandgap at 1.67 and 1.96 eV, respectively.¹⁷ An absorption coefficient of $\sim 1.1 \times 10^5 \text{ cm}^{-1}$ was estimated at a wavelength of 500 nm using an integrating sphere on MBI films with an average film thickness of 250 nm as determined from AFM measurements. Considering the roughness of MBI

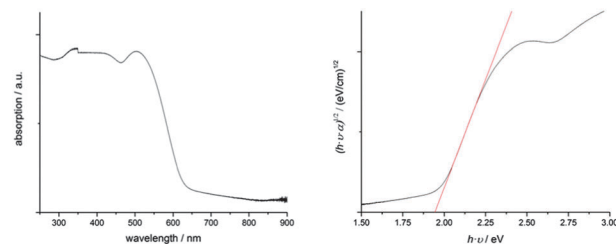


Fig. 2 Absorption spectra and Tauc plot of MBI (298 K).

films, this value is in good agreement with the value given by Park *et al.* and is of the same order of magnitude as determined for MAPbI.^{3,10}

XRD patterns of thin films, prepared *via* spin coating techniques using the solvents THF or DMF were recorded in Bragg-Brentano geometry and show good agreement when compared with the pattern calculated from single crystal data (Fig. 3) demonstrating a high degree of phase purity in the new material.

Minor differences in the intensity of the peaks may be caused by preferred orientation effects of the hexagonal material in such thin films. Rietveld refinements of powder patterns give results comparable to the single crystal data.

Summarizing, we have elucidated the correct crystal structure of $(\text{CH}_3\text{NH}_3)_3\text{Bi}_2\text{I}_9$ for the first time using single crystal measurements of this highly absorbing iodobismuthate. Even though the composition and its applicability for perovskite like hybrid solar cells would suggest similarities to $\text{CH}_3\text{NH}_3\text{PbI}_3$, MBI does not contain corner sharing octahedra normally observed in perovskite materials but isolated $\text{Bi}_2\text{I}_9^{3-}$ anions.[‡]

With the synthesis procedure described in this study we were able to show, that it is possible to obtain phase pure and highly crystalline $(\text{CH}_3\text{NH}_3)_3\text{Bi}_2\text{I}_9$ thin films in contrast to previous work.

Integration of our MBI films in solar cell architectures following the interfaces developed for MAPbI devices, we were able to achieve a sizable open circuit voltage of ~ 800 mV.¹⁸ However cell efficiencies were low, most probably due to the rough morphology of the MBI layer and the energetic mismatch

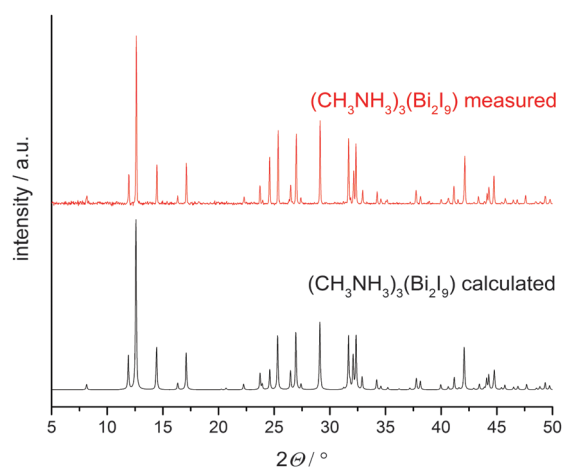


Fig. 3 XRD patterns of $(\text{CH}_3\text{NH}_3)_3\text{Bi}_2\text{I}_9$ calculated from single crystal data (black) compared to a measured thin film (red).



within the stack structure, since it is optimized for MAPbI. Based on the structural observations reported in this work, it will be crucial to attain deeper insights into the mechanism of the charge carrier transport within MBI and optimize interfaces. Since the optical absorption coefficient of MBI and the open circuit voltage are high, MBI is worth further investigations raising the hope to offer a good alternative for lead containing absorbers. However, further work is necessary to improve processing and contacting in order to explore its full potential.

We hope that our data provide a precise basis for future studies targeting deeper insights and understanding into band structure and transport properties of this new family of Bi-based HOIP materials.

Notes and references

‡ Crystal data for $(\text{CH}_3\text{NH}_3)_3\text{Bi}_2\text{I}_9$: $\text{C}_3\text{H}_{18}\text{Bi}_2\text{I}_9\text{N}_3$, $M_r = 1656.26$, hexagonal $P6_3/mmc$ (No. 194), $a = 8.5843(12) \text{ \AA}$, $c = 21.690(4) \text{ \AA}$, $V = 1384.2(5) \text{ \AA}^3$, $Z = 2$, $D_c = 3.974 \text{ g cm}^{-3}$, 764 independent reflections observed, $R_1 = 0.0453$ ($I > 2\sigma(I)$), $wR_2 = 0.1250$ (all data), and GOF = 0.865; CCDC 1433118 ($\text{CH}_3\text{NH}_3)_3\text{Bi}_2\text{I}_9$.

- 1 L. Martiradonna, *Nat. Mater.*, 2014, **13**, 837.
- 2 G. Hodes, *Science*, 2013, **342**, 317–319.
- 3 M. a. Green, A. Ho-Baillie and H. J. Snaith, *Nat. Photonics*, 2014, **8**, 506–514.

- 4 S. Kazim, M. K. Nazeeruddin, M. Grätzel and S. Ahmad, *Angew. Chem.*, 2014, **126**, 2854–2867.
- 5 D. B. Mitzi, *Synthesis, Structure, and Properties of Organic-Inorganic Perovskites and Related Materials*, John Wiley & Sons, 1994.
- 6 T. M. Koh, K. Fu, Y. Fang, S. Chen, T. C. Sum, N. Mathews, S. G. Mhaisalkar, P. P. Boix and T. Baikie, *J. Phys. Chem. C*, 2014, **118**, 16458–16462.
- 7 A. Kojima, M. Ikegami, K. Teshima and T. Miyasaka, *Chem. Lett.*, 2012, **41**, 397–399.
- 8 N. J. Jeon, J. H. Noh, W. S. Yang, Y. C. Kim, S. Ryu, J. Seo and S. Il Seok, *Nature*, 2015, **517**, 476–480.
- 9 K. Eckhardt, Bleifreie Licht Absorbierende Verbindung, Verfahren Zu Deren Herstellung Und Deren Verwendung in Optoelektronischen Bauelementen, n.d., 10 2015 213 100.9.
- 10 B.-W. Park, B. Philippe, X. Zhang, H. Rensmo, G. Boschloo and E. M. J. Johansson, *Adv. Mater.*, 2015, **9**, 6806–6813.
- 11 J. Berry, T. Buonassisi, D. A. Egger, G. Hodes, L. Kronik, Y.-L. Loo, I. Lubomirsky, S. R. Marder, Y. Mastai and J. S. Miller, *et al.*, *Adv. Mater.*, 2015, **27**, 5102–5112.
- 12 R. Jakubas, J. Zaleski and L. Sobczyk, *Ferroelectrics*, 1990, **108**, 109–114.
- 13 R. Jakubas and L. Sobczyk, *Phase Transitions*, 1990, **20**, 163–193.
- 14 T. Kawai, A. Ishii, T. Kitamura, S. Shimanuki, M. Iwata and Y. Ishibashi, *J. Phys. Soc. Jpn.*, 1996, **65**, 1464–1468.
- 15 C. C. Stoumpos, C. D. Malliakas and M. G. Kanatzidis, *Inorg. Chem.*, 2013, **52**, 9019–9038.
- 16 C. Feldmann, *Z. Kristallogr.*, 2001, **216**, 465–466.
- 17 N. J. Podraza, W. Qiu, B. B. Hinojosa, H. Xu, M. A. Motyka, S. R. Phillpot, J. E. Baciak, S. Trolrier-McKinstry and J. C. Nino, *J. Appl. Phys.*, 2013, **114**, 033110.
- 18 J. Burschka, N. Pellet, S.-J. Moon, R. Humphry-Baker, P. Gao, M. K. Nazeeruddin and M. Grätzel, *Nature*, 2013, **499**, 316–319.

